Citation: Clin Transl Sci (2017) 10, 509–519; doi:10.1111/cts.12486

ARTICLE

Prediction of Transporter-Mediated Drug-Drug Interactions for Baricitinib

Maria M. Posada[1,*], Ellen A. Cannady[1], Christopher D. Payne[1], Xin Zhang[1], James A. Bacon[1], Y. Anne Pak[1], J. William Higgins[1,3], Nazila Shahri[2], Stephen D. Hall[1] and Kathleen M. Hillgren[1]

Baricitinib, an oral selective Janus kinase 1 and 2 inhibitor, undergoes active renal tubular secretion. Baricitinib was not predicted to inhibit hepatic and renal uptake and efflux drug transporters, based on the ratio of the unbound maximum eliminating-organ inlet concentration and the *in vitro* half-maximal inhibitory concentrations (IC_{50}). *In vitro*, baricitinib was a substrate for organic anion transporter (OAT)3, multidrug and toxin extrusion protein (MATE)2-K, P-glycoprotein (P-gp), and breast cancer resistance protein (BCRP). Probenecid, a strong OAT3 inhibitor, increased the area under the concentration-time curve from time zero to infinity ($AUC_{[0-\infty]}$) of baricitinib by twofold and decreased renal clearance to 69% of control in healthy subjects. Physiologically based pharmacokinetic (PBPK) modeling reproduced the renal clearance of baricitinib and the inhibitory effect of probenecid using the *in vitro* IC_{50} value of 4.4 μM. Using ibuprofen and diclofenac *in vitro* IC_{50} values of 4.4 and 3.8 μM toward OAT3, 1.2 and 1.0 $AUC_{(0-\infty)}$ ratios of baricitinib were predicted. These predictions suggest clinically relevant drug-drug interactions (DDIs) with ibuprofen and diclofenac are unlikely.

Clin Transl Sci (2017) **10**, 509–519; doi:10.1111/cts.12486; published online on 27 July 2017.

Study Highlights

WHAT IS THE CURRENT KNOWLEDGE ON THE TOPIC?
✔ Mechanistic modeling has been widely used for the prediction of enzyme-mediated DDIs. Few examples are available to validate the use of *in vitro* data and mechanistic modeling for the prediction of renal transporter-mediated DDIs.

WHAT QUESTION DID THIS STUDY ADDRESS?
✔ Will the clearance of baricitinib depend on active secretion by OAT3 and will the plasma exposure of baricitinib be affected by the co-administration of drugs, commonly used in define? Will baricitinib affect the exposure of drugs whose clearances depend on transporters?

WHAT THIS STUDY ADDS TO OUR KNOWLEDGE
✔ Baricitinib is actively secreted by OAT3 and its interactions with OAT3 inhibitors can be predicted using *in vitro* inhibition data and PBPK modeling.

HOW THIS MIGHT CHANGE CLINICAL PHARMACOLOGY OR TRANSLATIONAL SCIENCE
✔ *In vitro* transporter data and PBPK modeling can help design and focus drug development plans on studies that have the greatest value.

Baricitinib (formerly LY3009104 or INCB028050) is an oral selective Janus kinase (JAK) 1 and 2 inhibitor being developed for the treatment of inflammatory diseases, such as rheumatoid arthritis (RA). Established therapies for RA include corticosteroids, disease-modifying antirheumatic drugs (such as methotrexate), JAK inhibitors, biologics (such as tumor necrosis factor-α or and interleukin 6 inhibitors), and nonsteroidal anti-inflammatory drugs (NSAIDs).[1] Consequently, it is important to understand the drug-drug interaction (DDI) potential for baricitinib, especially with commonly used NSAIDs, such as ibuprofen and diclofenac.

Baricitinib is predominantly eliminated unchanged in urine (70% of dose) with a renal clearance of ~11 L/h.[2] Baricitinib is a weak base (pKa 4.0), neutral at pH 7.4, and could, therefore, be secreted by the basolaterally expressed organic cation transporter 2 (OCT2, SLC22A2) and at the apical membrane by the multidrug and toxin extrusion protein transporters 1 and 2-K (MATE1 and MATE2-K, SLC47A1 and A2) or, alternatively, by the basolaterally expressed organic anion transporters 1 or 3 (OAT1 or OAT3, SLC22A6 and 8). OAT3 has been shown to transport both anionic and cationic compounds, such as furosemide, 6 beta-hydroxycortisol, cimetidine, and oseltamivir.[3–7] Thus, the identification of the transporter(s) responsible for active tubular secretion *a priori* is challenging and must be achieved with *in vitro* renal uptake and efflux transporter assays. Such data can be integrated within a physiologically based pharmacokinetic (PBPK) model to determine the potential for clinical DDIs with concomitant therapies that inhibit renal secretion. A number of drugs commonly used in RA have the potential to elicit DDIs at the level of renal secretion, including the NSAIDs, ibuprofen and diclofenac that inhibit OAT3 *in vitro*. This paper

[1]Eli Lilly and Company, Indianapolis, Indiana, USA; [2]inVentiv Health Clinical, La Jolla, California, USA; [3]Current address: Organovo Inc., San Diego, California, USA.
*Correspondence: Maria M. Posada (mmposada@lilly.com)
Received 27 January 2017; accepted 30 May 2017; published online on 27 July 2017. doi:10.1111/cts.12486

describes a series of *in vitro* studies, clinical evaluations, and PBPK modeling approaches to predict transporter-mediated DDI with baricitinib as either a perpetrator or victim drug.

MATERIALS AND METHODS

Materials

Baricitinib, LSN335984 (P-glycoprotein [P-gp] inhibitor), and ^{13}C-baricitinib (internal standard) were synthesized in-house. The ^{14}C-baricitinib was obtained from ABC Laboratories (Columbia, MO). The ^{14}C-metformin, ^{3}H-pravastatin, and ^{3}H-rosuvastatin were purchased from American Radiolabeled Chemicals (St. Louis, MO). The ^{3}H-vinblastine, ^{3}H-estrone-3-sulfate, ^{3}H-cholecystokinin fragment 26-33 amide, ^{3}H-1-methyl-4-phenylpyridinium, and ^{14}C-para-aminohippuric acid were purchased from Perkin Elmer (Boston, MA). All other chemicals were of analytical grade and purchased from commercial sources.

Stably transfected HEK-PEAK cells expressing OCT1, OCT2, OATP1B1, OATP1B3, OAT1, OAT3, or vector control (VC), were generated using previously described methods.[8] HEK cells transiently transfected with MATE1, MATE2-K, or VC were purchased from Corning Life Sciences (Transporto cells, Bedford, MA). Madin-Darby canine kidney (MDCK)-multidrug resistance protein (MDR)1 cells were obtained from The Netherlands Cancer Institute (Amsterdam, The Netherlands). MDCK-breast cancer resistance protein (BCRP) cells were generated at Absorption Systems (Exton, PA).

In vitro uptake and inhibition studies

Uptake by HEK cells transfected with OCT1, OCT2, OAT1, OAT3, OATP1B1, OATP1B3, MATE1, or MATE2-K was quantified using either ^{14}C-baricitinib or liquid chromatography-tandem mass spectrometry (LC-MS/MS) with ^{13}C-baricitinib as an internal standard. Time-course and kinetic studies were conducted on transporters that were positive in the initial screen for substrate.

Time-course substrate studies were conducted in HEK-PEAK VC and OAT3 cells at 37°C for up to 10 min with 10 μM ^{14}C-baricitinib (0.44 μCi/mL) in the presence and absence of probenecid (100 μM). Concentration-dependent studies were conducted with 1 min incubations, using 0.25–50 μM baricitinib (with 0.01–0.44 μCi/mL ^{14}C-baricitinib). Time-course accumulation of baricitinib (0.25 μM) in HEK control and MATE2-K cells was conducted at 37°C for up to 10 min in the presence and absence of cimetidine (100 μM) with LC-MS/MS. HEK-MATE2-K cells were incubated in 40 mM ammonium chloride for 20 min before addition of baricitinib to reverse the inwardly driven proton gradient of these transporters by intercellular acidification. HEK-MATE2-K and control cells were incubated with varying concentrations of baricitinib (0.05–50 μM) for 0.5 min at 37°C.

The inhibition of the OAT3-mediated uptake of ^{14}C-baricitinib was determined at 0.5 μM baricitinib (below the Michaelis-Menten constant [K_m]) in the presence of probenecid (0.1–100 μM), ibuprofen (0.1–100 μM), or methotrexate (MTX; 2.5–500 μM) for 1 min at 37°C. The inhibition of the MATE2-K-mediated uptake of baricitinib at 0.25 μM baricitinib (below the K_m) for 0.5 min at 37°C in the presence of cimetidine (0–100 μM), pyrimethamine (0–100 μM), or probenecid (0–200 μM) was performed as described above.

Bidirectional transport assessment for ^{14}C-baricitinib (5 μM, 0.21 μCi/mL) was conducted in MDCK-MDR1 cells as described[9–11] in the absence and presence of 5 μM LSN335984 (P-gp-specific inhibitor), 50 μM verapamil, and 50 μM quinidine. Bidirectional transport for baricitinib (5 μM) was conducted in MDCK-BCRP cell monolayers using a similar method as described in ref. 9 in the absence and presence of 0.5 μM Ko143, 2 μM fumitremorgin C, and 15 μM GF120918.

Data analysis

Kinetic parameters for OAT3-mediated baricitinib uptake were calculated using nonlinear regression (Phoenix, Pharsight Corporation, Mountain View, CA), according to Eq. (1):

$$\text{Total Uptake Rate} = \frac{(V_{max} \times S)}{(K_m + S)} + (K_d \times S) \quad (1)$$

where V_{max} (pmol/min/mg of protein) is the maximal velocity, S (μM) is the baricitinib concentration, K_m (μM) is the Michaelis-Menten constant, and K_d (μL/min/mg of protein) is the passive diffusion clearance determined by measuring uptake of baricitinib into vector control cells.

The MATE2-K-mediated uptake of baricitinib was obtained by subtracting passive diffusion measured in the VC cells at each concentration from the uptake in MATE2-K transfected cells and fitted to Eq. (2):

$$\text{MATE2} - \text{K Mediated Uptake Rate} = \frac{(V_{max} \times S)}{(K_m + S)} \quad (2)$$

The half-maximal inhibitory concentration (IC_{50}) values were determined by nonlinear regression using Eq. (3):

$$\%\ \text{activity} = \text{Min} + \frac{\text{Max} - \text{Min}}{\left(1 + \left(\frac{[I]}{IC_{50}}\right)^{slope}\right)} \quad (3)$$

where the % activity is the percentage of activity of substrate in relation to the uptake without an inhibitor added; Min and Max are the lowest and highest percentage activity in the presence of inhibitor; [I] the inhibitor concentration; and slope is the slope factor of the curve. Values were corrected for passive diffusion determined by substrate accumulation into VC cells. Where complete inhibition was not achieved, a maximum inhibitor concentration, the Min, was set to zero. DDI indices (unbound inhibitor concentration $[I_u]/IC_{50}$) and R values were calculated as described by the International Transporter Consortium.[12]

The baricitinib P-gp-mediated and BCRP-mediated intrinsic clearance (CL_{int}) were calculated by first subtracting the passive apparent permeability (Papp) from the basolateral to apical (B to A) Papp (without inhibitor). The resulting Papp was multiplied by the surface area of the insert (1.13 cm^2) and divided by the number of cells in the incubation (0.5×10^6).

Table 1 Physicochemical and biochemical parameters used in the PBPK models

	Baricitinib		Probenecid		Ibuprofen		Diclofenac	
Input parameter	**Value**	**Source**	**Value**	**Source**	**Value**	**Source**	**Value**	**Source**
Molecular weight (g/mol)	371.42		285.4	ChemSpider (Royal Society of Chemistry)	206.28	ChemSpider (Royal Society of Chemistry)	296.15	ChemSpider (Royal Society of Chemistry)
fu	0.5	Measured using equilibrium dialysis[14]	0.12	[15]	0.018	[16]	0.003	[17,18]
LogP	−0.189	Calculated with Chemaxon	2.44	Calculated Chemaxon	4.13	[19]	4.51	[19]
B/P	1.26	Measured in human mass balance study	0.55	Simcyp predicted	0.55	Simcyp predicted	0.55	Simcyp predicted
pK_a	4.0 (basic)	Measured using a potentiometric method	3.4 (acidic)	[20]	4.42 (acidic)	[19]	3.99 (acidic)	[19]
Fa	0.8	Calculated from human mass balance study	1	[20]	1	[21]	1	[17]
k_a (h^{-1})	1.2	Fitted to match clinical data	0.56	[22]	1.52	[23]	6	Value calculated as 1/gastric emptying time
t_{lag} (h)	–	–	–	–	0.1	[23]	–	–
Kp scalar	2.3	Fitted to match clinical data	0.5	Fitted to match clinical data	–	–	–	–
Clearance/F (L/h)	–	–	0.73 (oral)	Calculated as described in methods	5 (oral)	[23]	Clearance = 20[a] (i.v.)	[17,24]
OAT3 K_m (μM)	5.54	Measured as described in Methods section	–	–	–	–	–	–
OAT3 V_{max} (pmol/min/10^6 cells)	70.76	Measured as described in Methods section						
MATE2-K K_m (μM)	32.4	Measured as described in Methods section	–	–	–	–	–	–
MATE2-K V_{max} (pmol/min/10^6 cells)	657.5	Measured as described in Methods section						
P-gp CL_{int} (μL/min/10^6 cells)	2.7	Measured as described in Methods section	–	–	–	–	–	–
BCRP CL_{int} (μL/min/10^6 cells)	0.8	Measured as described in Methods section						
Additional plasma clearance (L/h)	2.5	$CL_{total} - CL_{renal}$	–	–	–	–	–	–
IC_{50} OAT3 (μM)	–	–	4.41	Measured	4.46	Measured	3.6	[25]

BCRP, breast cancer resistance protein; B/P, blood to plasma concentration ratio; CL_{int}, intrinsic clearance; F, systemic bioavailability; Fa, fraction absorbed from intestinal lumen into gut wall; fu, fraction unbound in plasma; IC_{50}, half-maximal inhibitory concentration; ka, first-order absorption rate constant; K_i, inhibition constant; K_m, Michaelis-Menten constant; Kp, tissue-to-plasma coefficient; LogP, log of octanol/water partition coefficient; MATE, multidrug and toxin extrusion protein; OAT, organic anion transporter; PBPK, physiologically based pharmacokinetic modeling; P-gp, P-glycoprotein; t_{lag}, time before start of drug absorption; V_{max}, Maximum uptake velocity.
[a]For diclofenac only, i.v. clearance is presented, rather than clearance/F. The clearance reported in the reference was scaled using body weight to match the Simcyp population.

Clinical study

An open-label, two-period, fixed-sequence study was conducted in healthy subjects to investigate the effects of OAT3 inhibition by probenecid on the pharmacokinetics (PKs) of baricitinib (Clinicaltrials.gov: NCT01937026). Subjects received a single dose of 4-mg baricitinib on day 1 after an overnight fast, followed by 1,000 mg probenecid b.i.d. on days 3 through 7. On day 5, after an overnight fast, a second single dose of 4-mg baricitinib was administered ~1 h after the morning dose of probenecid. Subjects were not taking any drugs or herbal supplements. The study protocol was approved by an institutional review

board and was conducted in accordance with the Declaration of Helsinki and Good Clinical Practice guidelines. All subjects provided written informed consent prior to participating. Safety was assessed by physical examinations, clinical laboratory evaluations (hematology, urinalysis, and biochemistry panels), vital signs assessments, and safety electrocardiograms and monitoring of treatment-emergent adverse events (AEs).

Blood samples were collected predose and 0.5, 1, 2, 4, 6, 8, 12, 16, 24, 36, and 48 h after the days 1 and 5 baricitinib doses. An additional 72-h sample was taken after the day 5 administration. Blood samples for PK analysis of probenecid were collected predose and 1, 2, 4, 6, 24, and 48 h after the morning dose of probenecid on day 5. On days 1 and 5, urine samples were collected predose and pooled for periods 0–6, 6–12, 12–24, 24–36, and 36–48 h after the baricitinib dose; an additional sample was collected during the period 48–72 h after the day 5 baricitinib dose. Plasma and urine samples were analyzed using validated LC-MS/MS methods for baricitinib with ranges from 0.20–200 ng/mL in plasma, 10.0–10,000 ng/mL in urine, and for probenecid with a range from 1.00 and 500 μg/mL.

The terminal half-life was determined from 0.693/elimination rate constant (ke). The ke was determined by log-linear regression of the terminal points of the plasma concentration time curve. The area under the concentration-time curve from zero to infinity ($AUC_{[0-\infty]}$) was determined by the trapezoidal rule with extrapolation to infinity using the ke (Phoenix). The peak plasma concentration (C_{max}) was the maximum concentration observed at time (t_{max}). The apparent clearance (CL/F) was calculated from dose/$AUC_{[0-\infty]}$, and renal clearance (CL_r) from the amount of drug excreted in urine (Ae)/$AUC_{[0-\infty]}$.

Baricitinib PK parameter estimates for $AUC_{(0-\infty)}$, C_{max}, and CL_r were log-transformed and analyzed using a mixed-effects analysis-of-variance model, which included treatment (baricitinib alone or baricitinib + probenecid) as the fixed effect and subject as the random effect. The ratio of least squares (LS) geometric means for baricitinib + probenecid (test treatment) compared with baricitinib alone (reference treatment) and the 90% confidence interval (CI) of the ratio were reported. The t_{max} for baricitinib was analyzed using a CI based on a nonparametric approach, as described by Hahn and Meeker.[13] Estimates of the median difference and 90% CI for the difference between baricitinib + probenecid (test treatment) and baricitinib alone (reference treatment) were calculated.

PBPK modeling

All simulations were performed using Simcyp version 13.2 (Simcyp, Sheffield, UK). Full PBPK models for baricitinib, probenecid, ibuprofen, and diclofenac were developed using measured and predicted physicochemical and biological data (**Table 1**).[14–25] Simulations were all performed using North European white men from the ages of 22–63 years.

Baricitinib

The model was set up with perfusion rate-limited distribution between blood and tissues, except for the kidney, which was set up as a permeability-limited tissue. The multicompartment mechanistic kidney model was used to incorporate the glomerular filtration and active renal secretion of baricitinib.[26] The Cockcroft-Gault predicted glomerular filtration rate (GFR) and the fraction unbound (fu; 0.5) were used to calculate the filtration clearance of baricitinib (3.5 L/h); the geometric mean GFR was 7.0 L/h in this population. The active secretion of baricitinib was modeled using the *in vitro* measured V_{max} and K_m values for OAT3 and MATE2-K, and intrinsic clearances of P-gp and BCRP. The relative activity factor (RAF) value was set to 1 for all transporters (OAT3, MATE2-K, P-gp, and BCRP), assuming there is no difference in activity between the *in vitro* systems and *in vivo*. Baricitinib was modeled using first-order absorption, with an absorption rate constant (ka) estimated from the plasma concentration-time profiles. The fraction absorbed (Fa) and the bioavailability (F) were assumed to be 0.8 given that 20% of the dose was found as parent compound in feces in the human mass balance study (Clinicaltrials.gov NCT01299285) and the low hepatic and intestinal extraction. The volume of distribution at steady-state was estimated using the plasma concentration-time profiles. The baricitinib model was verified over a range of doses from 2–20 mg q.d. for 10 days.[2]

Probenecid

The absorption of probenecid was simulated using the first-order absorption model.[22] The fu in plasma at the C_{max} of probenecid is estimated from the nonlinear relationship between plasma concentration and fu.[15] The clearance of probenecid after oral administration (CL/F) was calculated from the average concentration at steady-state ($C_{ave,ss}$) and the rate of administration of probenecid (2,000 mg/day) using Eq. (4).[27] The $C_{ave,ss}$ of probenecid at steady-state was calculated using Eq. (5),[27] where $C_{min,ss}$ is the minimum and $C_{max,ss}$ is the maximum concentration at steady-state.

$$Clearance = \frac{Rate\ of\ Administration}{C_{ave,\ ss}} \tag{4}$$

$$C_{ave} = \frac{(C_{max,\ ss} - C_{min,\ ss})}{Ln\left(\frac{C_{max,\ ss}}{C_{min,\ ss}}\right)} \tag{5}$$

Ibuprofen

Ibuprofen was based on a published model[25] modified to use first-order absorption based on the reported PK parameters.[23]

Diclofenac

Diclofenac was based on the physicochemical properties and PK parameters of an immediate release formulation based on data collected from the literature.[17–19,24] The fraction absorbed was assumed to be 1 and the absorption rate constant (ka) was assumed to be determined by gastric emptying rate. The IC_{50} of diclofenac for OAT3 was obtained from a previous study, using pemetrexed as the substrate[25] and assuming there is no substrate-dependent inhibition for OAT3.

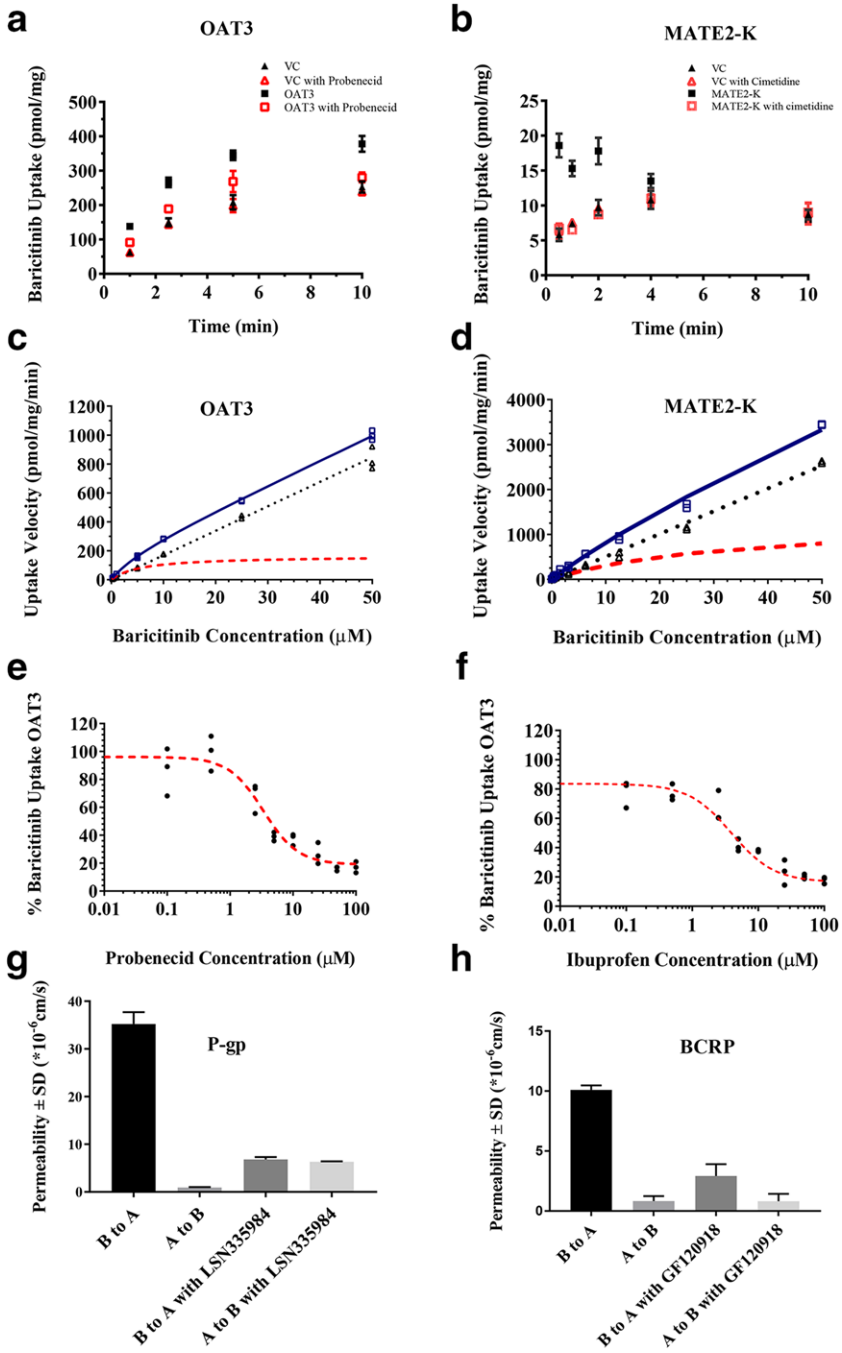

Figure 1 *In vitro* uptake studies (**a**) Time-dependent uptake of 10 μM ^{14}C-baricitinib (0.44 μCi/mL) in vector control (VC; ▲), VC + 100 μM probenecid (△), organic anion transporter (OAT)3 (■), and OAT3 + 100 μM probenecid (□) in transfected HEK-PEAK cells. Data are presented as mean ± SD ($N = 3$ separate wells). (**b**) Time-dependent uptake of 10 μM baricitinib in VC (▲), VC + 100 μM cimetidine (△), multidrug and toxin extrusion protein (MATE)2-K (■), and MATE2-K + 100 μM cimetidine (□) transfected HEK-PEAK cells. Data are presented as mean ± SD ($N = 3$ separate wells). (**c**) Concentration-dependent uptake of ^{14}C-baricitinib in VC (△) and OAT3 (□) transfected HEK-PEAK cells treated for 1 min ($N = 3$ separate wells). The solid line represents the fitted total uptake, the dotted line represents the fitted uptake into VC, and the dashed line represents the predicted OAT3-mediated uptake. (**d**) Concentration-dependent uptake of baricitinib in VC and MATE2-K transfected HEK-PEAK cells treated for 1 min ($N = 3$ separate wells). The solid line represents the fitted total uptake, the dotted line represents the fitted uptake into VC, and the dashed line represents the predicted MATE2-K-mediated uptake. (**e**) Inhibition of the OAT3-mediated uptake of ^{14}C-baricitinib (0.5μM) by probenecid (0.1–100 μM). The solid line represents the fitted uptake and circles represent the individual observations ($N = 3$ separate wells). (**f**) Inhibition of the OAT3-mediated uptake of ^{14}C-baricitinib (0.5 μM) by ibuprofen (0.1–100 μM). The solid line represents the fitted uptake and circles represent the individual observations ($N = 3$ separate wells). (**g**) Bidirectional transport (A to B and B to A) of baricitinib in Madin-Darby canine kidney (MDCK)-multidrug resistance protein 1, in the presence and absence of 5 μM LSN335984 (P-glycoprotein-specific inhibitor). (**h**) Bidirectional transport (A to B and B to A) of baricitinib in MDCK-breast cancer resistance protein (BCRP), in the presence and absence of 15 μM of GF120918 (BCRP inhibitor).

Table 2 Calculation of DDI index for the different *in vitro* inhibitors with baricitinib as a substrate

Transporter	Inhibitor	IC_{50} (μM) (individual experiments) Mean ± SD	IC_{50} (μM) mean	$C_{max\ inhibitor}$ [I] (μM)	$C_{max\ unbound\ inhibitor}$ [I_u] (μM)	DDI index ([I_u]/IC_{50})
OAT3	Probenecid	3.38 ± 0.6	4.41	245[a]	22.1	5.0
		5.43 ± 1.2				
	Ibuprofen	5.01 ± 1.2	4.46	300[b]	3.0	0.7
		3.91 ± 0.0				
	Diclofenac[c]	3.7 (21%)[c]	3.7[c]	6.3[d]	0.03	0.01
	Methotrexate	116 ± 15.4	92.2	1.1[e]	0.6	0.01
		68.4 ± 13.2				
MATE2-K	Cimetidine	1.64 ± 0.5	5.1	9.9[f]	7.9	1.6
		8.34 ± 2.02				
		5.18 ± 0.52				
	Pyrimethamine	0.27 ± 0.04	0.25	0.9[g]	0.1	0.5
		0.22 ± 0.04				
	Probenecid	NI	NI	245[a]	22.1	NA
		NI				

C_{max}, maximum observed concentration; DDI, drug-drug interaction; I, steady-state maximum observed concentration; I_u, unbound steady-state maximum observed concentration; IC_{50}, half-maximal inhibitory concentration; Inhib, inhibitor; MATE, multidrug and toxin extrusion protein; NA, not applicable; NI, no inhibition; OAT, organic anion transporter.
[a]1 g oral dose, 91% plasma bound.[29]
[b]800 mg oral dose, 99% plasma bound.[30]
[c]Diclofenac IC_{50} was taken from published study, using pemetrexed as a substrate.[25] The value is reported as mean percent coefficient of variation.
[d]100 mg oral dose, 99.7% bound to plasma.[30]
[e]15 mg s.c. dose, 46% plasma bound.[30]
[f]400 mg oral dose, 20% plasma bound.[31]
[g]25 mg oral dose, 87% plasma bound.[32]
The DDI index was calculated to assess the potential for inhibitors to have clinically relevant interactions via OAT3 and MATE2-K. Inhibition of baricitinib uptake at each transporter was determined experimentally for individual inhibitors; IC_{50} values were calculated using nonlinear regression analysis. Unbound C_{max} was estimated from published values of C_{max} and unbound fraction for the respective inhibitor at commonly prescribed doses. DDI index >0.1 indicates that a clinical DDI study is recommended.

DDI simulations

The interaction between baricitinib and OAT inhibitors was assumed to occur at the level of the basolateral uptake transporter OAT3 using the values in **Table 1**.[14–25] It was also assumed that probenecid, ibuprofen, and diclofenac did not inhibit the apical efflux transporters (P-gp, BCRP, and MATE2-K; https://didb.druginteractioninfo.org/).[28] In the simulations, probenecid was administered as a dose of 1,000 mg b.i.d., ibuprofen as 800 mg q.i.d, and diclofenac as 100 mg b.i.d. Inhibitors were administered from day 1 through day 5 and baricitinib was administered as a single dose on day 3.

RESULTS

In vitro

The uptake of baricitinib into OCT1, OCT2, OATP1B1, OATP1B3, OAT1, and MATE1 transfected cells was similar to control cells, indicating that baricitinib was not a substrate of these transporters (see **Supplementary Figures S1** and **S2**).

Uptake of baricitinib into OAT3-transfected cells was approximately double that of control cells after a 1-min incubation, and was inhibited by probenecid, indicating baricitinib is a substrate of OAT3 (**Figure 1a**). The uptake of baricitinib into MATE2-K cells was approximately three times greater than control cells at 0.5 min, and was inhibited by cimetidine, indicating that baricitinib is a substrate of MATE2-K (**Figure 1b**). The uptake of baricitinib into OAT3 cells was concentration-dependent and saturable (**Figure 1c**). The average (two separate experiments with three replicates each) K_m and V_{max} of baricitinib were 5.54 μM (5.33 ± 1.21; 5.74 ± 0.56) and 176.9 pmol/min/mg protein (189.5 ± 27.10; 164.3 ± 7.97). The uptake of baricitinib into MATE2-K cells was concentration-dependent and saturable (**Figure 1d**) with K_m of 32.4 ± 6.1 μM and V_{max} of 1315 ± 129 pmol/min/mg protein. The average (two or three separate experiments with three replicates) OAT3 IC_{50} values of probenecid, ibuprofen, and methotrexate were 4.41, 4.46, and 92.2 μM, respectively (**Table 2**[25,29–32]; representative IC_{50} graphs for probenecid and ibuprofen, **Figure 1e and 1f**, respectively). The average MATE2-K IC_{50} values for cimetidine (two separate experiments with two replicates each) and pyrimethamine (two separate experiments with two replicates each) were 5.05 and 0.23 μM, respectively (**Table 2**[25,29–32]). Probenecid did not inhibit the MATE2-K-mediated baricitinib transport. DDI indices for probenecid and ibuprofen were 5.01 and 0.67, suggesting a clinically relevant inhibition of OAT3. Cimetidine and pyrimethamine indices were 1.57 and 0.49, also suggesting a clinically relevant inhibition of MATE2-K (**Table 2**[25,29–32], representative IC_{50} graphs in **Supplementary Figure S3**).

In MDCK-MDR1 cells, the A to B Papp of baricitinib was $0.9 \cdot 10^{-6}$ cm/s and the B to A $35.2 \cdot 10^{-6}$ cm/s. This efflux ratio of 39.1 was reduced to 1, 2, and 6 in the presence of LSN335984, verapamil, and quinidine, respectively, indicating baricitinib is a P-gp substrate (**Figure 1g** and

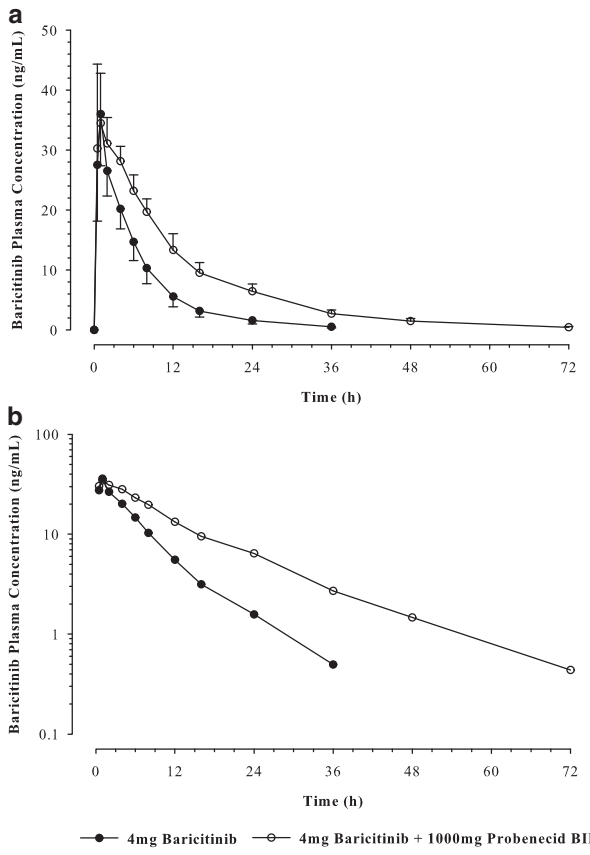

Figure 2 (**a**) Linear scale and (**b**) log scale arithmetic mean concentration vs. time profiles for baricitinib following administration of a single 4-mg dose with (○) or without (●) 1,000 mg b.i.d. probenecid in 18 healthy subjects. Error bars show one-sided SD.

Supplementary Figure S4). The apparent passive permeability (Papp) of baricitinib was $6.6 \cdot 10^{-6}$ cm/s. In the MDCK-BCRP cells, the A to B Papp of baricitinib was $0.83 \cdot 10^{-6}$ cm/s and the B to A Papp $10.1 \cdot 10^{-6}$ cm/s. This efflux ratio of 12.1 was decreased to 5.8, 4.8, and 3.6 by Ko143, fumitremorgin C, and GF120918, respectively; indicating baricitinib is a substrate of BCRP (**Figure 1h** and **Supplementary Figure S4**).

No clinically relevant inhibition of uptake and efflux transporters by baricitinib is expected when therapeutic plasma concentrations of baricitinib are considered (**Supplementary Table S1**). This is supported by the lack of interaction of baricitinib with MTX and digoxin in clinical studies.[33]

Clinical study

Eighteen healthy white men aged 22–63 years, and with a body mass index 21.1–28.5 kg/m^2, entered and completed the clinical study. Plasma baricitinib concentration-time profiles after administration of 4 mg of baricitinib alone or in combination with probenecid are shown in **Figure 2** and the corresponding PK parameters in **Table 3**. In the presence of probenecid, the baricitinib $AUC_{(0-\infty)}$ was doubled, the CL/F was 51% lower, the CL_r was 69% lower, and the half-life 63% longer (**Table 3**).

Probenecid co-administration resulted in statistically significant differences in $AUC_{(0-\infty)}$ and CL_r, given that the 90% CIs for the ratios of geometric LS means did not contain 1. Probenecid co-administration showed no effect in C_{max}, with the 90% CI for the ratio of geometric LS means completely contained within the boundary of 0.80–1.25. There was no statistically significant difference in t_{max}.

The mean C_{max} for probenecid was 145μg/mL and the trough plasma concentration (C_{min}) was 88μg/mL. The median probenecid t_{max} was 2 h postdose, confirming that maximal exposure coincided with the maximal baricitinib exposure (baricitinib having a median t_{max} of 1 h postdose, and probenecid having been dosed 1 h before baricitinib). Baricitinib and probenecid were well tolerated. All drug-related treatment-emergent AEs were mild and no discontinuations were due to AEs.

PBPK modeling

The baricitinib model reproduced the observed concentration plasma profiles (**Figure 3a**) after a 4-mg oral dose with observed/predicted C_{max} and $AUC_{(0-\infty)}$ equal to 1. The CL_r (10.6 L//h predicted, 11 L/h observed) and renal excretion profiles (**Figure 3b**) were well predicted. The model accurately predicted dose linear changes in $AUC_{(0-t)}$ and C_{max} (**Figure 3c,d**) and no changes in renal and apparent clearance after multiple dosing.[2] Because the bottom-up model built using *in vitro* transporter data (OAT3, MATE2K, P-gp, and BCRP) reproduced the observed renal secretory clearance of baricitinib, after accounting for the amount of protein per million cells, no additional scaling factors were added (RAF = 1). If the model had not reproduced the observed renal secretory clearance, a scaling factor would have been required to fit the active secretion as previously done.[25,44] For pemetrexed, a small relative activity factor (RAF) of 5.3 was used, but there were slight differences in methodologies. Others have also reported small RAF values for OAT1 (0.64), OAT2 (7.3), and OAT3 (4.1).[34]

The observed probenecid plasma concentrations were adequately reproduced by the model (**Figure 3e**) and the predicted C_{max} and $C_{ss,ave}$ were similar to the observed ones (**Table 4**[17,45]). The predicted C_{max} and $AUC_{(0-\infty)}$ values of ibuprofen were similar to the reported values[21] (**Table 4**[17,45]). For diclofenac, the predicted values were close to the observed ranges for C_{max} and $AUC_{(0-\infty)}$ following administration of an immediate release formulation[17] (**Table 4**[17,45]).

The model adequately reproduced the effect of probenecid on baricitinib, with a predicted $C_{max,ratio}$ (90% CI) of 1.17 (1.15–1.7) and an AUC_{ratio} (90% CI) of 1.95 (1.84–2.07). These predicted ratios were within 0.8 and 1.25-fold of the observed AUC ratio (90% CI) of 2.03 (1.91–2.16) and observed $C_{max,ratio}$ (90% CI) 1.03 (0.940–1.13; **Table 4**[17,45]). The predicted AUC_{ratio} (90% CI) of 1.24 (1.22–1.26) and $C_{max,ratio}$ of 1.07 (1.06–1.08) with ibuprofen indicated low clinical relevance for this interaction (**Table 4**[17,45]). The OAT3 IC_{50} value for ibuprofen (4.46 μM) using baricitinib as a substrate was similar to the previously measured value with pemetrexed (4.15 μM),[25] confirming the assumption that OAT3 inhibition is substrate independent. Therefore, the IC_{50} for diclofenac, which was measured with pemetrexed (3.7 μM)[25] was used for modeling the interaction with baricitinib and

Table 3 Baricitinib PK parameter estimates and statistical analysis in healthy subjects following single doses of 4 mg baricitinib with or without 1,000 mg b.i.d. probenecid

Parameter	Baricitinib Only (N = 18)	Baricitinib + Probenecid (N = 18)	Ratio of Geometric LS Means Baricitinib + Probenecid:Baricitinib Only) (90% CI)[d]	
	Geometric Mean (CV)			
$AUC_{(0-\infty)}$ (ng·h/mL)	236 (22)	480 (14)	2.03 (1.91, 2.16)	
C_{max} (ng/mL)	36.2 (22)	37.3 (20)	1.03 (0.940, 1.13)	
CL/F (L/h)	16.9 (22)	8.33 (14)	NA	
CLr (L/h)	11.0 (29)	3.43 (20)	0.313 (0.289, 0.339)	
$Ae_{(0-48)}$ (mg)[a]	2.60 (0.399)	1.57 (0.191)	NA	
t1/2 (h)[b]	7.28 (4.87-9.26)	11.9 (9.61-13.9)	NA	
	Median (Range)		Median Difference (Baricitinib + Probenecid: Baricitinib) (Approximate 90% CI)	P-value
tmax (h)[c]	1.00 (0.50-2.00)	1.00 (0.50-4.00)	0.00 (-0.0167, 0.0167)[e]	0.608

$Ae_{(0-48)}$ = amount of drug excreted within time 0 to 48 h post-dose; $AUC_{(0-\infty)}$ = area under the concentration-time curve from zero to infinity; CL/F = apparent clearance; CL_r = renal clearance; C_{max} = maximum observed concentration; N = number of subjects; $t_{1/2}$ = half-life; t_{max} = time of C_{max}.
[a]Arithmetic mean (standard deviation).
[b]Geometric mean (range).
[c]Median (range).
[d]Analyzed using the following mixed-effects analysis-of-variance model: Log(PK) = treatment + subject + random error, where subject was a random effect.
[e]Analyzed using Wilcoxon signed rank test.

diclofenac, resulting in $AUC_{(0-\infty)}$ and C_{max} ratios of 1.0, predicting no clinically relevant interaction (**Table 4**[17,45]).

DISCUSSION

In the current study, it was determined that the renal tubular secretion of baricitinib is not mediated by OCT2, OAT1, or MATE1, but is dependent on the basolaterally expressed OAT3 and the apically expressed P-gp, BCRP, and MATE2-K transporters. OAT3 transports drugs, such as pemetrexed, furosemide, and oseltamivir[3,4,25] and inhibition of OAT3 decreases the renal clearance and increases plasma exposure of several drugs.[4] Probenecid decreases the clearance of oseltamivir by 32%[6] and CL_r of furosemide by 66%, whereas increasing furosemide AUC by 2.6-fold.[36] We measured the inhibition potency of the OAT3 inhibitors probenecid, MTX, and ibuprofen toward the OAT3-mediated uptake of baricitinib *in vitro*. The DDI index recommended by the International Transporter Consortium,[37] was used to rank their inhibition potential to cause clinically relevant DDIs (DDI index >0.1). *In vitro*, ibuprofen (0.67) and probenecid (5.01) had DDI indices suggesting potential for clinical OAT3-mediated DDIs.

Because baricitinib was an OAT3 substrate *in vitro* and probenecid had the highest DDI index, a baricitinib-probenecid clinical DDI study was performed in healthy volunteers. The steady-state concentrations of probenecid produced maximal OAT3 inhibition, as evidenced by reduction of CL_r of baricitinib to GFR. In the presence of probenecid, CL_r and CL/F of baricitinib decreased 69% and 51%, respectively, whereas the $AUC_{(0-\infty)}$ of baricitinib doubled. Probenecid inhibits multiple transporters (e.g., OAT2, OAT3, OAT4, OATP1B3, and multidrug resistance-associated protein [MRP]2, MRP3, MRP4, and MRP5 to a lesser extent).[38–42] Therefore, a clinical probenecid study alone does not sufficiently identify the transporter responsible for the active secretion. However, the combination of *in vitro* and clinical results suggests the effect of probenecid on baricitinib clearance is due to OAT3 inhibition.

Because probenecid decreased the active secretion of baricitinib, the effects of OAT3 inhibitors with less inhibition potential, specifically ibuprofen and diclofenac,[25] were investigated using PBPK modeling. Transporter-mediated interactions can be challenging to predict when intracellular concentrations are the driving force of transport and inhibition. However, for OAT3, the free plasma concentration drives the substrate and inhibition potential, thus removing a large uncertainty in the prediction. A combination of *in vitro* transporter parameters and clinical PK data were leveraged to inform parameters of the baricitinib and probenecid models. This resulted in accurate predictions of key PK parameters of baricitinib and probenecid, $AUC_{(0-\infty)}$ and C_{max}, and the effect of probenecid on baricitinib, which were within 0.8–1.25 of the observed values (**Table 4**[17,45]). Subsequently, PBPK models were built for ibuprofen and diclofenac to predict the inhibition potential for the OAT3-mediated active secretion of baricitinib. The ibuprofen model was previously verified for the OAT3 substrate pemetrexed and provided good concordance of the observed and predicted clinical data; predicted changes in $AUC_{(0-\infty)}$ and C_{max} were between onefold and 1.1-fold of those observed.[25] The accuracy of the predictions of probenecid on baricitinib and ibuprofen on pemetrexed[25] gives confidence that *in vitro* inhibition data can predict clinical interactions at OAT3. The models predicted that coadministration of ibuprofen would not cause clinically relevant changes in the $AUC_{(0-\infty)}$ and C_{max} of baricitinib. The predicted increase in baricitinib $AUC_{(0-\infty)}$ (24%) is within the variability of observed PK data, and is unlikely to be clinically relevant. For diclofenac, predicted $AUC_{(0-\infty)}$ and C_{max} values for baricitinib administered alone or with diclofenac were identical, indicating that diclofenac is unlikely to influence baricitinib exposure. OAT3 IC_{50} values for ibuprofen were generated with baricitinib and pemetrexed as substrate and were equivalent, supporting the assumption of the lack

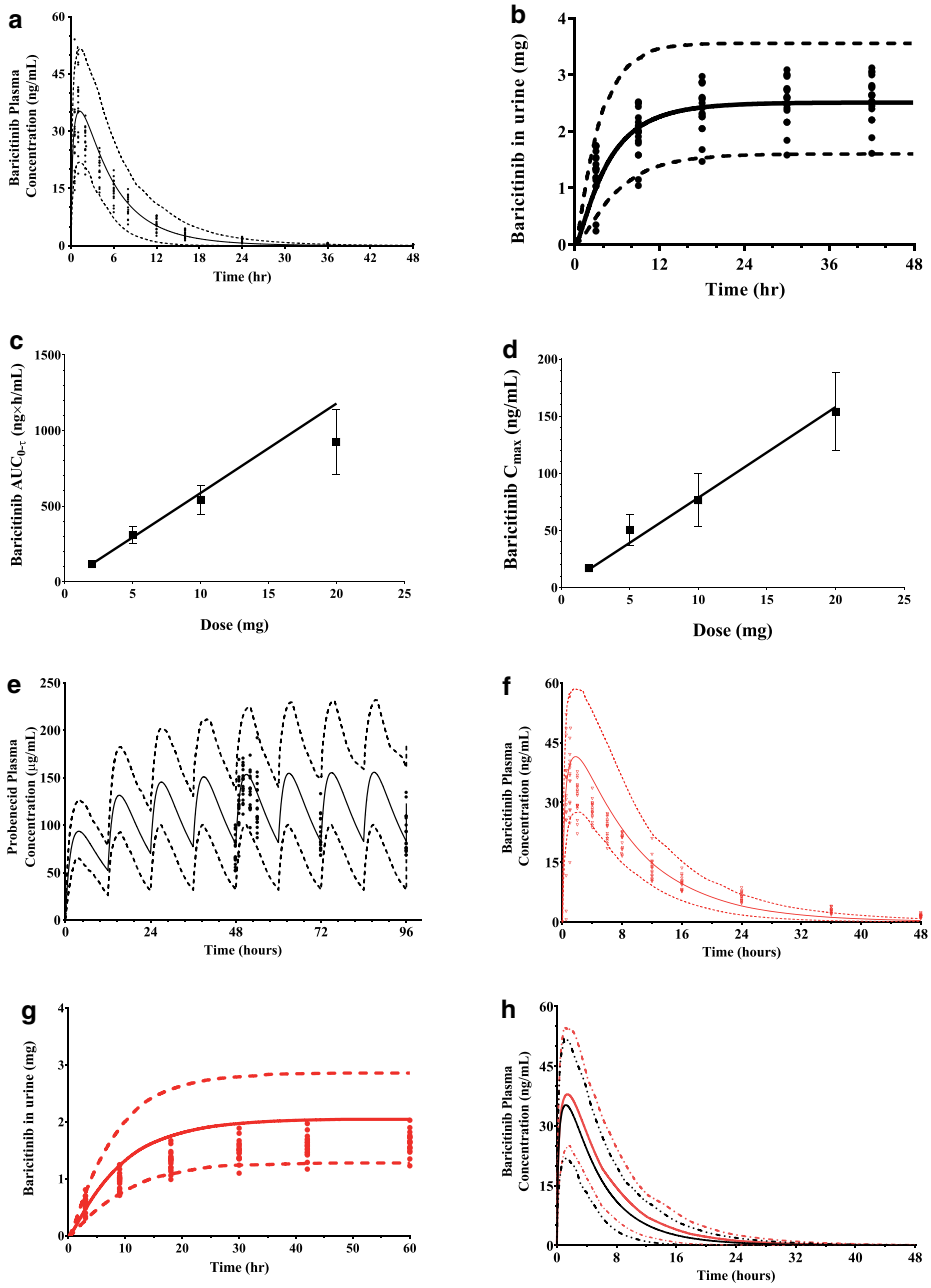

Figure 3 (**a**) Predicted and individual observed plasma baricitinib concentration vs. time profiles following a single oral dose of 4-mg baricitinib. Points represent the observed values. The solid line represents the mean predicted concentration, and the dashed lines represent the predicted 5th and 95th percentiles. (**b**) Cumulative urine excretion of baricitinib following a single oral dose of 4-mg baricitinib. Points represent the observed data. The solid black line represents the predicted mean cumulative amount of baricitinib excreted in urine. The dash lines represent the predicted 5th and 95th percentiles. (**c**) Effect of increasing dose on baricitinib area under the concentration-time curve $(AUC)_{(0-t),ss}$ after q.d. dosing for 10 days. The squares represent the observed data[2] and the line represents the predicted data. Observed data are presented as geometric mean ± SD. (**d**) Effect of increasing dose on baricitinib peak plasma concentration steady-state ($C_{max,ss}$) after q.d. dosing for 10 days. The squares represent the observed data[2] and the line represents the predicted data. (**e**) Predicted and observed plasma probenecid concentration vs. time profiles following b.i.d. dosing of 1,000 mg probenecid. Circles represent the observed data. The solid line represents the mean predicted concentration, and the dash lines represent the predicted 5th and 95th percentiles. (**f**) Observed and predicted plasma concentration vs. time profiles for baricitinib in the presence of 1,000 mg probenecid. Open triangles represent the observed baricitinib concentrations in the presence of probenecid. The solid red line represents the predicted mean concentration of baricitinib in the presence of probenecid. The dashed lines represent the predicted 5th and 95th percentiles. (**g**) Cumulative urine excretion of baricitinib following a single oral dose of 4-mg baricitinib in the presence of probenecid. Red circles represent the observed data. The solid red line represents the predicted mean cumulative amount of baricitinib excreted in urine in the presence of probenecid. The dashed lines represent the predicted 5th and 95th percentiles. (**h**) Predicted plasma concentration vs. time profiles for baricitinib in the presence (red) and absence (black) of 800-mg ibuprofen. The solid lines represent the mean predicted concentrations and the dashed lines represent the 5th and 95th percentiles.

Table 4 Observed and predicted AUC and C_{max} for baricitinib, probenecid, ibuprofen and diclofenac.

Compound	Parameter	Observed Mean (CV)	Predicted Geometric Mean (5-95% CI)	Observed/ Predicted
Baricitinib	C_{max} (ng/mL)	36.2 (22)	34.9 (33.3 – 36.7)	1.0
	AUC(0-∞) (ng·h/mL)	236 (22)	230 (215 – 247)	1.0
Probenecid (1,000 mg BID)	C_{max} (μg/mL)	145	160 (150 – 169)	0.9
	$C_{ss,ave}$ (μg/mL)	115	116 (94 – 139)	1.0
Ibuprofen (800 mg QID)	C_{max} (μg/mL)	55.6 (24)[a]	52.8 (50.1 – 55.6)	1.1
	AUC (μg·h /mL)	218 (23)[a]	183 (170 – 196)	1.2
Diclofenac(100 mg BID)	C_{max} (μg/mL)	1.2 – 3.6[b]	2.7	–
	AUC (μg·h/mL)	2.7 – 4.4[b]	3.0	–
Baricitinib (+/- Probenecid)	AUC ratio(90% CI)[c]	2.03(1.91-2.16)	1.95 (1.84-2.07)	1.0
Baricitinib (+/- Probenecid))	C_{max} ratio(90% CI)[d]	1.03 (0.940, 1.13)	1.17 (1.15-1.7)	0.9
Baricitinib (+/- Ibuprofen)	AUC ratio(90% CI)[c]	NA	1.24 (1.22-1.26)	NA
Baricitinib (+/- Ibuprofen)	C_{max} ratio(90% CI)[d]	NA	1.07 (1.06-1.08)	NA
Baricitinib (+/-Diclofenac)	AUC ratio (90% CI)[c]	NA	1.00 (1.00-1.00)	NA
Baricitinib (+/- Diclofenac)	C_{max} ratio(90% CI)[d]	NA	1.00 (1.00-1.00)	NA

$AUC_{(0-\infty)}$ = area under the concentration-time curve (AUC) from zero to infinity; CI = confidence interval; C_{max} = maximum observed concentration; $C_{ss,ave}$ = average concentration at steady state.
[a]Published mean[45]
[b]Published ranges[17]
[c]AUC ratio = AUC of baricitinib in the presence of the inhibitor (probenecid, ibuprofen or diclofenac) / AUC of baricitinib alone
[d]Cmax ratio = Cmax of baricitinib in the presence of the inhibitor (probenecid, ibuprofen or diclofenac) / Cmax of baricitinib alone

of substrate dependence and application of this approach to other OAT3 substrates.

Transport by OAT3 is expected to determine the plasma concentration and renal clearance of baricitinib.[5,42] In the model, it was assumed that OAT3 was a unidirectional transporter, responsible for influx into cells without reabsorption back into plasma, which is consistent with the low calculated log of octanol/water partition coefficient of -0.189 and poor passive permeability in MDCK cells suggested by slow Papp.[10] However, the involvement of other transporters for basolateral efflux of baricitinib cannot be ruled out. The assumption of lack of involvement of basolateral efflux may not be appropriate for other transporters, such as OCTs, which are facilitative transporters and may not be the rate limiting step in renal secretion.[35,43]

Baricitinib is a substrate for the efflux transporters P-gp, BCRP, and MATE2-K. Additional apical efflux mechanisms (i.e., MRPs and OAT4) could also exist, although these pathways have not been investigated for baricitinib. In a clinical DDI study with baricitinib and cyclosporine, a P-gp and BCRP inhibitor, there was a 30% decrease in renal secretory clearance of baricitinib,[33] supporting the hypothesis that BCRP and P-gp are not the major apical efflux mechanisms. However this rests on the unproven assumption that a single 600 mg dose of cyclosporine completely inhibits P-gp and BCRP. Specific clinically potent inhibitors for the apical transporters are needed to fully differentiate the involvement of each transporter in CL_r *in vivo*. However, inhibition of apical transporters does not necessarily increase systemic exposure of OAT3 substrates. For example, following administration of probenecid to healthy volunteers, the systemic plasma concentrations of 6 beta-hydroxycortisol, a substrate of OAT3, MATE1, and MATE2-K, increased but administration of pyrimethamine (MATE1 and MATE2-K inhibitor) had no effect.[5,42] This likely reflects differences in basolateral efflux efficiencies among OAT3 substrates.

In conclusion, the PBPK models developed to quantify the potential inhibition of OAT3-mediated secretion of baricitinib successfully reproduced the observed data. This approach allowed translation of *in vitro* data to predict and confirm clinical DDI potential with probenecid, which subsequently enabled additional model development to predict other OAT3-mediated DDIs with ibuprofen and diclofenac.

Acknowledgments. This work was funded by Eli Lilly and Company and Incyte Corporation. The authors wish to acknowledge the investigators and subjects who participated in this study, as well as the following individuals: Jamie Scism-Bacon and Karen Turpin of Eli Lilly and Company for project management support; William V. Williams of Incyte Corp. for oversight of the conduct of the methotrexate clinical trial; David Radtke of Eli Lilly and Company for assistance with producing figures for this paper.

Author Contributions. M.P., E.C., C.P., X.Z., J.B., Y.P., J.H., N.S., S.H., and K.H. wrote the manuscript. M.P., E.C., C.P., X.Z., J.B., Y.P., J.H., N.S., S.H., and K.H. designed the research. M.P., J.B., Y.P., and J.H. performed the research. M.P. and J.H. contributed new reagents/ analytic tools. M.P., E.C., X.Z., J.B., Y.P., J.H., and K.H. analyzed the data.

Conflict of Interest. Posada, Cannady, Bacon, Hall, Pak, Payne, Zhang, and Hillgren are paid employees of Eli Lilly and Company. Posada, Cannady, Bacon, Hall, Hillgren, Pak, Payne, and Zhang have stock ownership/options in Eli Lilly and Company. Shahri was an employee of InVentive Health Clinical, and whose services were contracted by Eli Lilly and Company. Higgins is an employee of Organovo, Inc.

1. Tanaka, Y. Current concepts in the management of rheumatoid arthritis. *Korean J. Intern. Med.* **31**, 210–218 (2016).
2. Shi, J.G. *et al.* The pharmacokinetics, pharmacodynamics, and safety of baricitinib, an oral JAK 1/2 inhibitor, in healthy volunteers. *J. Clin. Pharmacol.* **54**, 1354–1361 (2014).
3. Hasannejad, H. *et al.* Interactions of human organic anion transporters with diuretics. *J. Pharmacol. Exp. Ther.* **308**, 1021–1029 (2004).
4. Burckhardt, G. Drug transport by organic anion transporters (OATs). *Pharmacol. Ther.* **136**, 106–130 (2012).
5. Imamura, Y. *et al.* 6β-Hydroxycortisol is an endogenous probe for evaluation of drug-drug interactions involving a multispecific renal organic anion transporter, OAT3/SLC22A8, in healthy subjects. *Drug Metab. Dispos.* **42**, 685–694 (2014).
6. Holodniy, M. *et al.* Pharmacokinetics and tolerability of oseltamivir combined with probenecid. *Antimicrob. Agents Chemother.* **52**, 3013–3021 (2008).
7. Imamura, Y. *et al.* Prediction of fluoroquinolone-induced elevation in serum creatinine levels: a case of drug-endogenous substance interaction involving the inhibition of renal secretion. *Clin. Pharmacol. Ther.* **89**, 81–88 (2011).
8. Godinot, N. *et al.* Cloning and functional characterization of the multidrug resistance-associated protein (MRP1/ABCC1) from the cynomolgus monkey. *Mol. Cancer Ther.* **2**, 307–316 (2003).
9. Sawada, G.A. *et al.* Chalcogenopyrylium dyes as inhibitors/modulators of P-glycoprotein in multidrug-resistant cells. *Bioorg. Med. Chem.* **16**, 9745–9756 (2008).
10. Raub, T.J., Lutzke, B.S., Andrus, P.K., Sawada, G.A. & Staton, B.A. Early preclinical evaluation of brain exposure in support of hit identification and lead optimization. (eds. Borchardt,R.T., Kerns,E.H., Hageman,M.J., Thakker,D.R. & Stevens,J.L.) 355–410 In: *Optimizing the "Drug-Like" Properties of Leads in Drug Discovery*. (Springer New York, New York, NY, 2006).
11. Sawada, G.A. *et al.* Increased lipophilicity and subsequent cell partitioning decrease passive transcellular diffusion of novel, highly lipophilic antioxidants. *J. Pharmacol. Exp. Ther.* **288**, 1317–1326 (1999).
12. Giacomini, K.M. & Huang, S.M. Transporters in drug development and clinical pharmacology. *Clin. Pharmacol. Ther.* **94**, 3–9 (2013).
13. Hahn, G.J. & Meeker, W.Q. Statistical intervals: A guide for practitioners. DOI:10.1002/9780470316771 (2011).
14. Zamek-Gliszczynski, M.J. *et al.* Validation of 96-well equilibrium dialysis with non-radiolabeled drug for definitive measurement of protein binding and application to clinical development of highly-bound drugs. *J. Pharm. Sci.* **100**, 2498–2507 (2011).
15. Emanuelsson, B.M., Beermann, B. & Paalzow, L.K. Non-linear elimination and protein binding of probenecid. *Eur. J. Clin. Pharmacol.* **32**, 395–401 (1987).
16. Lockwood, G.F., Albert, K.S., Szpunar, G.J. & Wagner, J.G. Pharmacokinetics of ibuprofen in man–III: plasma protein binding. *J. Pharmacokinet. Biopharm.* **11**, 469–482 (1983).
17. Davies, N.M. & Anderson, K.E. Clinical pharmacokinetics of diclofenac. Therapeutic insights and pitfalls. *Clin. Pharmacokinet.* **33**, 184–213 (1997).
18. Riess, W. *et al.* Pharmacokinetics and metabolism of the anti-inflammatory agent Voltaren. *Scand. J. Rheumatol. Suppl.* **22**, 17–29 (1978).
19. Avdeef, A., Berger, C.M. & Brownell, C. pH-metric solubility. 2: correlation between the acid-base titration and the saturation shake-flask solubility-pH methods. *Pharm. Res.* **17**, 85–89 (2000).
20. Cunningham, R.F., Israili, Z.H. & Dayton, P.G. Clinical pharmacokinetics of probenecid. *Clin. Pharmacokinet.* **6**, 135–151 (1981).
21. Davies, N.M. Clinical pharmacokinetics of ibuprofen. The first 30 years. *Clin. Pharmacokinet.* **34**, 101–154 (1998).
22. Selen, A., Amidon, G.L. & Welling, P.G. Pharmacokinetics of probenecid following oral doses to human volunteers. *J. Pharm. Sci.* **71**, 1238–1242 (1982).
23. Lötsch, J., Muth-Selbach, U., Tegeder, I., Brune, K. & Geisslinger, G. Simultaneous fitting of R- and S-ibuprofen plasma concentrations after oral administration of the racemate. *Br. J. Clin. Pharmacol.* **52**, 387–398 (2001).
24. Willis, J.V., Kendall, M.J., Flinn, R.M., Thornhill, D.P. & Welling, P.G. The pharmacokinetics of diclofenac sodium following intravenous and oral administration. *Eur. J. Clin. Pharmacol.* **16**, 405–410 (1979).
25. Posada, M.M. *et al.* Prediction of renal transporter mediated drug-drug interactions for pemetrexed using physiologically based pharmacokinetic modeling. *Drug Metab. Dispos.* **43**, 325–334 (2015).
26. Neuhoff, S. *et al.* Accounting for transporters in renal clearance: towards a mechanistic kidney model (Mech KiM). (eds. Sugiyama,Y. & Steffansen,B.) 155–177 In: *Transporters in Drug Development: Discovery, Optimization, Clinical Study and Regulation*. (Springer New York, New York, NY, 2013).
27. Rowland, M. & Tozer, T.N. *Clinical pharmacokinetics and pharmacodynamics: concepts and applications*. (Wolters Kluwer Health/Lippincott William & Wilkins, Philadelphia, PA, 2011).
28. Morrissey, K.M., Wen, C.C., Johns, S.J., Zhang, L., Huang, S.M. & Giacomini, K.M. The UCSF-FDA TransPortal: a public drug transporter database. *Clin. Pharmacol. Ther.* **92**, 545–546 (2012).
29. Pea, F. Pharmacology of drugs for hyperuricemia. Mechanisms, kinetics and interactions. *Contrib. Nephrol.* **147**, 35–46 (2005).
30. Brunton, L.L., Knollmann, B.C. & Hilal-Dandan, R. *Goodman & Gilman's The pharmacological basis of therapeutics, 13th Edition*. (Mc Graw-Hill Medical Publishers, Secaucus, NJ, 2011).
31. Jantratid, E. *et al.* Biowaiver monographs for immediate release solid oral dosage forms: cimetidine. *J. Pharm. Sci.* **95**, 974–984 (2006).
32. Ahmad, R.A. & Rogers, H.J. Pharmacokinetics and protein binding interactions of dapsone and pyrimethamine. *Br. J. Clin. Pharmacol.* **10**, 519–524 (1980).
33. Payne, C., Zhang, X., Shahri, N., Williams, W. & Cannady, E. AB0492 Evaluation of potential drug-drug interactions with baricitinib. *Ann. Rheum. Dis.* **74**(Suppl 2), 1063 (2015).
34. Mathialagan, S., Piotrowski, M.A., Tess, D.A., Feng, B., Litchfield, J. & Varma, M.V. Quantitative prediction of human renal clearance and drug-drug interactions of organic anion transporter substrates using in vitro transport data: a relative activity factor approach. *Drug Metab. Dispos.* **45**, 409–417 (2017).
35. Varma, M.V., Steyn, S.J., Allerton, C. & El-Kattan, A.F. Predicting clearance mechanism in drug discovery: Extended Clearance Classification System (ECCS). *Pharm. Res.* **32**, 3785–3802 (2015).
36. Vree, T.B., van den Biggelaar-Martea, M. & Verwey-van Wissen, C.P. Probenecid inhibits the renal clearance of frusemide and its acyl glucuronide. *Br. J. Clin. Pharmacol.* **39**, 692–695 (1995).
37. International Transporter Consortium *et al.* Membrane transporters in drug development. *Nat. Rev. Drug Discov.* **9**, 215–236 (2010).
38. Cutler, M.J. *et al.* In vitro and in vivo assessment of renal drug transporters in the disposition of mesna and dimesna. *J. Clin. Pharmacol.* **52**, 530–542 (2012).
39. Enomoto, A. *et al.* Interaction of human organic anion transporters 2 and 4 with organic anion transport inhibitors. *J. Pharmacol. Exp. Ther.* **301**, 797–802 (2002).
40. Jemnitz, K., Veres, Z., Tugyi, R. & Vereczkey, L. Biliary efflux transporters involved in the clearance of rosuvastatin in sandwich culture of primary rat hepatocytes. *Toxicol. In Vitro.* **24**, 605–610 (2010).
41. Reid, G. *et al.* Characterization of the transport of nucleoside analog drugs by the human multidrug resistance proteins MRP4 and MRP5. *Mol. Pharmacol.* **63**, 1094–1103 (2003).
42. Tahara, H., Kusuhara, H., Maeda, K., Koepsell, H., Fuse, E. & Sugiyama, Y. Inhibition of oat3-mediated renal uptake as a mechanism for drug-drug interaction between fexofenadine and probenecid. *Drug Metab. Dispos.* **34**, 743–747 (2006).
43. Kusuhara, H. & Sugiyama, Y. In vitro-in vivo extrapolation of transporter-mediated clearance in the liver and kidney. *Drug Metab. Pharmacokinet.* **24**, 37–52 (2009).
44. Hsu, V. *et al.* Towards quantitation of the effects of renal impairment and probenecid inhibition on kidney uptake and efflux transporters, using physiologically based pharmacokinetic modelling and simulations. *Clin. Pharmacokinet.* **53**, 283–293 (2014).
45. Small, R.E., Johnson, S.M. & Willis, H.E. Pharmacokinetic and taste evaluation of ibuprofen (Motrin) 800 mg tablets in extemporaneous solution. *J. Rheumatol.* **15**, 345–347 (1988).

Supplementary information accompanies this paper on the *Clinical and Translational Science* website. (http://onlinelibrary.wiley.com/journal/10.1111/(ISSN)1752-8062)